

## FULL-WAVE NUMERICAL MODELING OF NEAR-FIELD BEAM PROFILES AT 200 AND 700 GHZ

M. T. Chen<sup>2</sup>, C. E. Tong<sup>1</sup>, L. Chen<sup>3</sup>, S. Paine<sup>1</sup>, and R. Blundell<sup>1</sup>

<sup>1</sup>*Harvard-Smithsonian Center for Astrophysics,  
60 Garden St., Cambridge, MA 02138*

<sup>2</sup>*Institute of Astronomy and Astrophysics  
Academia Sinica, Taipei, Taiwan 115*

<sup>3</sup>*Harvard University, Cambridge, MA 02138*

### *Abstract*

A full-wave numerical method has been implemented to examine near-field beam profiles of antenna feeds at sub-millimeter wavelengths. Using a vectorial Green's function formulation, we have calculated the electromagnetic field distribution at the aperture of feed horns of 200 and 700 GHz. Beam pattern measurements in the near-field have been compared with the theoretical data projected to the measured plane. The calculated results agree well, in both amplitude and phase, with the measured data from feed horns used with SIS receivers developed for the Smithsonian Institution's Sub-Millimeter Array (SMA). We have also used this method to examine cross-polarization and beam distortion introduced by an off-axis parabolic mirror.

### *1. Introduction*

With noise temperatures of only a few times  $h\nu/k$ , sub-millimeter wavelength SIS receivers have been shown to provide quantum-limited sensitivity [1][2]. For the most sensitive receivers, the noise contribution arising from losses at the receiver input is often as high as that from other sources; the mixer and multiplied IF noise. In such systems, therefore, it is important to match the beam pattern emerging from the mixer feed to the optics of the remaining system

Two critical areas of the beam matching process have been identified. Firstly, submillimeter feed horns are generally very difficult to fabricate due to tight dimensional tolerances. Furthermore, possible defects introduced during machining may result in considerable deviation of the actual beam profile from the design goal. The radiated field pattern of the feed should therefore be accurately modeled. Secondly, lenses and mirrors making up the optical train may introduce distortion due to misalignment or aberration effects.

In the receiver development effort for the SMA, we have found it particularly important to accurately model and characterize the beam profile of the receiving system in order to fully utilize our low noise SIS receiver performance. We have developed a planar near-field scanning system to measure the beam profile of different feeds in the frequency range 200 - 700 GHz [3]. Furthermore, as a check on the scanned beam profiles, we have implemented a full-wave numerical method to model the measured beam profiles. This method, based on a vectorial Green's function, is adopted for its capability to simultaneously analyze amplitude and phase distributions. In this report, we present the preliminary comparisons of the theoretical data with near-field measurements for the 200 and 700 GHz corrugated horn feeds developed of the SMA receivers.

## II. Formulation

The numerical modeling is based on the well-known Green's function formulas [4][5]. A schematic diagram of the geometry for this type of calculation is shown in Fig.1. For simplicity, assuming a finite source located inside a closed surface S, the electromagnetic field outside the surface can be expressed as

$$\vec{E}(\vec{r}) = \frac{1}{2\pi} \int_S \frac{e^{ikR}}{R^2} \left[ ik - \frac{1}{R} \right] \cdot \vec{R} \times \left[ \hat{n}(\vec{r}_0) \times \vec{E}(\vec{r}_0) \right] \cdot dS \quad (1)$$

where  $k$  is the propagation constant,  $\hat{n}$  is the normal vector of the surface element  $dS(\vec{r}_0)$ , and  $\vec{R} = \vec{r} - \vec{r}_0$ .

To apply this formulation to our measured beam profile, we assume an ideal field distribution across the feed aperture. Thus, on a spherical surface bounded by the aperture and centered at the apex, the E-field amplitude distribution is a zero-order Bessel function and the phase of the electric field is constant [6]. Taking the beam axis as the z-axis, the direction of the field is perpendicular to the surface normal and is either oriented along the x- or y-axis, depending on the polarization. The electric field is assumed to be zero outside the aperture radius. In principle, starting from this initial field one can calculate the E-field on subsequent surfaces at arbitrary positions outside the feed according to Eq.(1). A square mesh with dimensions slightly larger than the aperture is created to model the initial field. The resolution of the mesh is adjusted empirically until satisfactory convergence of the data is achieved. A target mesh is created in the scanning plane with a dimension determined from the measured dynamic range. Other mesh sizes are implemented at positions of interest, for example, in the plane of a reflecting surface, along the line of propagation. A computer program, based on Eq.(1), then carries out the field summations to obtain a final vector-field distribution in the plane of interest.

The same formulation can be applied in a time-reversed sense by taking the complex conjugate of Eq.(1). In this case, the scanned data becomes the initial field, and the feed

aperture becomes the target plane of interest. This type of modeling can provide a direct verification of the quality of the feed.

### ***III. Experimental Arrangement***

A submillimeter planar near-field range is used to measure beam profiles to be compared with the numerical data. Two measurements have been performed in the context of this work; (a) Determination of the beam profile of a 200 GHz corrugated feed horn, designed for use with the lowest frequency SMA receivers [7], and (b) Determination of the beam profile in front of a test cryostat housing a 700 GHz corrugated feed horn with SIS mixer. In the later setup, the horn is arranged to illuminate a 90 degree off-axis parabolic mirror in the cryostat. Schematics of the experimental setup for these two experiments are shown as Figs. 2a and 2b, respectively.

In order to eliminate any intervening windows or IR filters that may truncate or distort the measured beam profile, the 200 GHz measurement is performed at room temperature. In this experiment a varactor frequency doubler, pumped by a Gunn oscillator at 93.5 GHz, is connected to the feed horn under test. The total radiated power is about 1mW. A harmonic mixer equipped with an open wave guide feed and pumped by a microwave synthesizer, is mounted on the scanner used to sample the beam profile. The distance between the scan plane and horn aperture is 125 mm. A dynamic range in excess of 30 dB is obtained in defining a scan plane 72 mm in extent. Data is sampled at 61x61 points along the axes, x and y, that define the scan plane.

Referring to Fig. 2b, the experimental setup for the 700 GHz measurement is similar to that reported previously [8]. However, in order to increase the dynamic range of the system, the signal source is made up of a phase-locked Gunn oscillator and a waveguide harmonic generator. The probe used is a WR-1.5 open waveguide with a cut-off frequency of 400 GHz. With a DSB receiver noise temperature of about 370K, a dynamic range of about 35 dB is achieved in the scan plane, 30 mm across. In this measurement, data is sampled at 63 points along each direction. The distance from the center of the mirror to the horn aperture is 58.5 mm, to the dewar window 105.5 mm, and to the scan plane 300 mm.

### ***IV. Results and Discussion***

Figure 3a shows the two-dimensional measured data from the near-field scanning of the 200 GHz corrugated feed horn at 187 GHz. The amplitude contours are in dB and the phase contours are in radian relative to the center of the scan plane. In our experimental setup, the scan plane is mechanically aligned to be normal to the axis of propagation. The alignment is accurate to within about 2 degrees. Since the scan plane is centered at the position of peak power, determined from a preliminary scan, its center is not necessarily

coincident with the beam axis in the measurement. This arrangement has caused the measured amplitude and phase contours to be off-center. The first step of data processing, therefore, is to relocate the beam axis and the center of the aperture with respect to the scan plane coordinates.

An initial calculation is carried out to reverse propagate the beam from the scan plane to a parallel plane at the feed aperture. In the calculation result we assume the position of peak power to be at the center of the feed aperture. Next, the measured amplitude is fitted using a two-dimensional quadratic equation on the scan plane. The maximum of the fitted equation is then taken as the center point of the data set. The beam axis is then defined as the line between this center point and the aperture center. A new plane covering the feed horn aperture is then created with its normal parallel to the beam axis. Finally, a second calculation is performed to reverse propagate the beam from the scan plane back to the new plane. Figure 3b presents the final modeling contours of the aperture field of the 200 GHz corrugated feed at 187 GHz. This data set is compared to the Bessel function field model of the aperture field of corrugated feeds. An RMS phase deviation of 16 degree is obtained. When a complex overlap integral is performed to measure the effectiveness of the modeling, we obtain a coefficient of 0.89.

In the case of modeling the beam profile of 700 GHz receiver, we start with an ideal Bessel function distribution at the aperture of the feed horn. The numerical code is used to propagate the radiated field at 660 GHz from the feed horn to the surface of a 90 degree off-axis parabolic mirror. Upon reflection, the tangential component of the incident electrical field along the mirror surface reverses direction. The reflected field is then numerically propagated to the cryostat window, then subsequently to the scan plane. The results of the modeling are compared to measured data in Fig.4 and Fig.5 at 660 GHz. As shown in Fig. 4, the E-plane cut, which is normal to the plane of incidence, is symmetrical both for the measured and theoretical data sets. In contrast, the distortion introduced by the 90 degree off-axis mirror is clearly visible in the H-plane cut. Comparisons of the amplitude data in both cuts indicate that the beam is slightly out of focus. This is attributed to a mis-alignment of the mirror in the cryostat. The optimized RMS deviations of the measured amplitude and phase from the modeling are 1.7 dB and 12 degree, respectively, for the E-plane cut, and 1.2 dB and 12 degree for the H-plane cut.

## ***V. Summary***

We have demonstrated the use of a full-wave numerical method, based on the Green's function formulas, to model the beam profiles for corrugated horn feeds developed for the SMA. This method, coupled with near-field scanning techniques, provides experimental verification of the design and manufacture of feed horns, and complete submillimeter receiver systems. Finally, the method may be applied to examine beam distortion and cross polarization effects introduced by focusing elements.

**References:**

---

- <sup>1</sup> R. Blundell and C.-Y. E. Tong, "Submillimeter Receivers for Radio Astronomy", *Proc. of the IEEE*, vol. 80, pp.1702-1720, November 1992.
- <sup>2</sup> R. Blundell, C.-Y. E. Tong, D. C. Papa, R. L. Leombruno, X. Zhang, S. Paine, J. A. Stern, H. G. LeDuc, and B. Bumble, "A Wideband Fixed-Tuned SIS Receiver for 200 GHz Operation", *IEEE Trans. Microwave Theory Tech.*, vol. 43, pp. 933-937, April 1995.
- <sup>3</sup> C.-Y. E. Tong, S. Paine, and R. Blundell, "Near-Field Characterization of 2-D Beam Patterns of Submillimeter Superconducting Receivers", in *Proc. 5th Int. Symp. Space Terahertz Tech.*, Ann Arbor, MI, pp. 660-673, May 1994.
- <sup>4</sup> J. D. Jackson, *Classical Electrodynamics*, Wiley, New York, 1975.
- <sup>5</sup> T. B. Hansen and A. D. Yaghjian, "Planar Near-Field Scanning in the Time Domain, Part 1: Formulation", *IEEE Trans. Antennas Propagat.*, vol. AP-42, pp. 1280-1291, September 1994.
- <sup>6</sup> P. J. B. Clarricoats and A. D. Olver, *Corrugated Horns for Microwave Antennas*, Peter Peregrinus Ltd., London, UK.
- <sup>7</sup> X. Zhang, "Design of Conical Corrugated Feed Horns for Wide-band High-frequency Applications", *IEEE Trans. Microwave Theory Tech.*, vol. 41, pp. 1263-1274, Aug. 1993.
- <sup>8</sup> C.-Y. E. Tong, R. Blundell, D. C. Papa, J. W. Barrett, S. Paine, X. Zhang, J. A. Stern, and H. G. LeDuc, "A Fixed Tuned Low Noise SIS Receiver for the 600 GHz Frequency Band", in *Proc. 6th Int. Symp. Space Terahertz Tech.*, pp.295-304, Pasadena, CA, March 1995.

$$\vec{E}(\vec{r}) = \frac{1}{2\pi} \int_S \frac{e^{ikR}}{R^2} \left[ ik - \frac{1}{R} \right] \cdot \vec{R} \times [\hat{n}(\vec{r}_0) \times \vec{E}(\vec{r}_0)] \cdot dS$$

$$\vec{R} = \vec{r} - \vec{r}_0$$

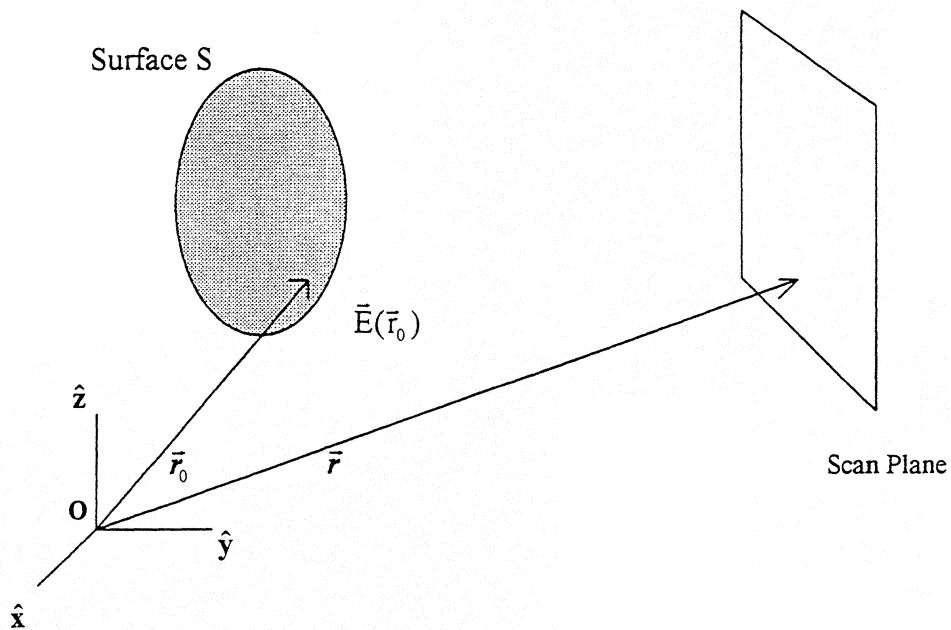


Figure 1: Schematic diagram of the calculation geometry.

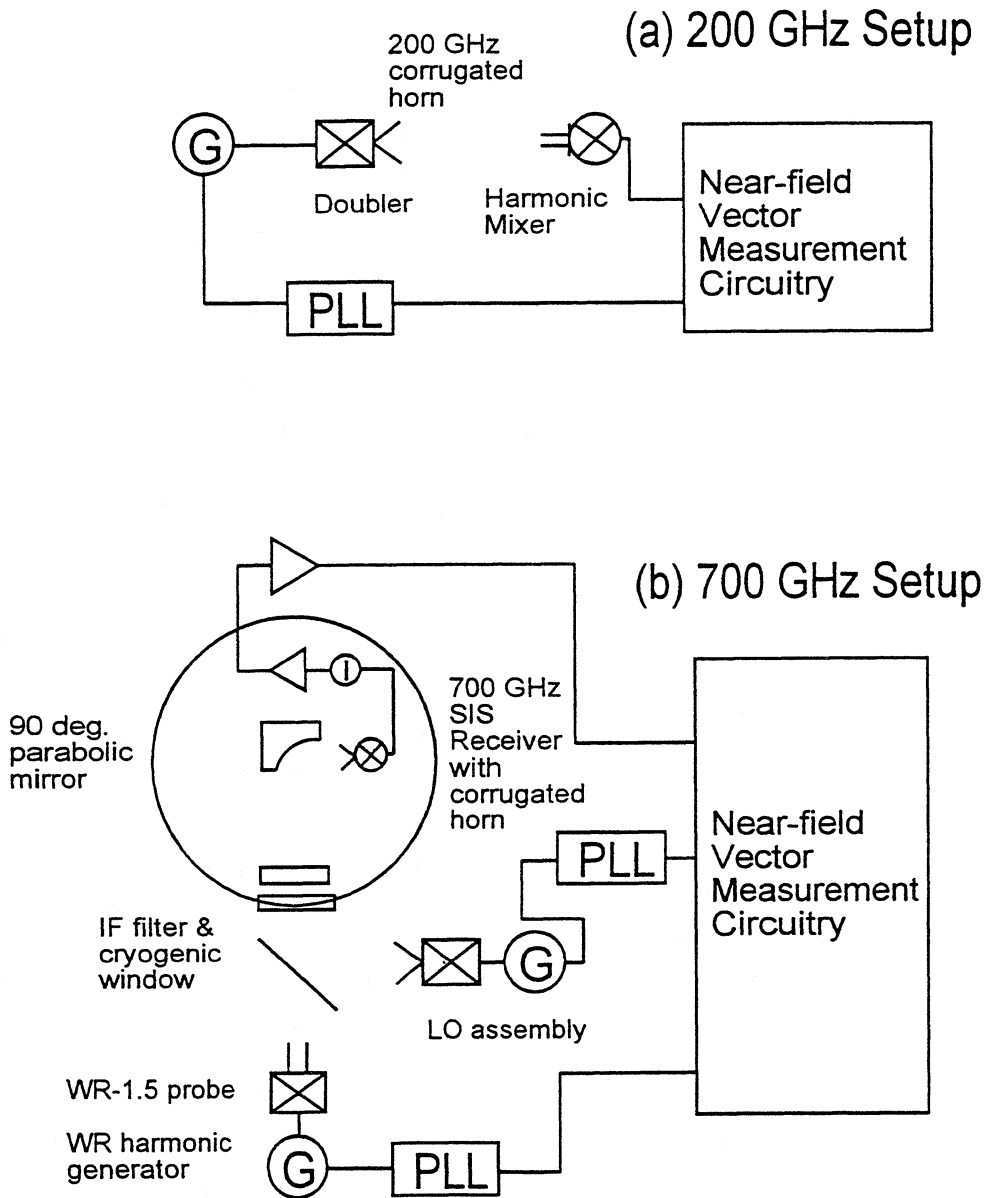


Figure 2: Schematic of the experimental setup for : a) the determination of the beam profile of a 200 GHz corrugated feed horn; b) the determination of the beam profile in front of a 700 GHz SIS receiver.

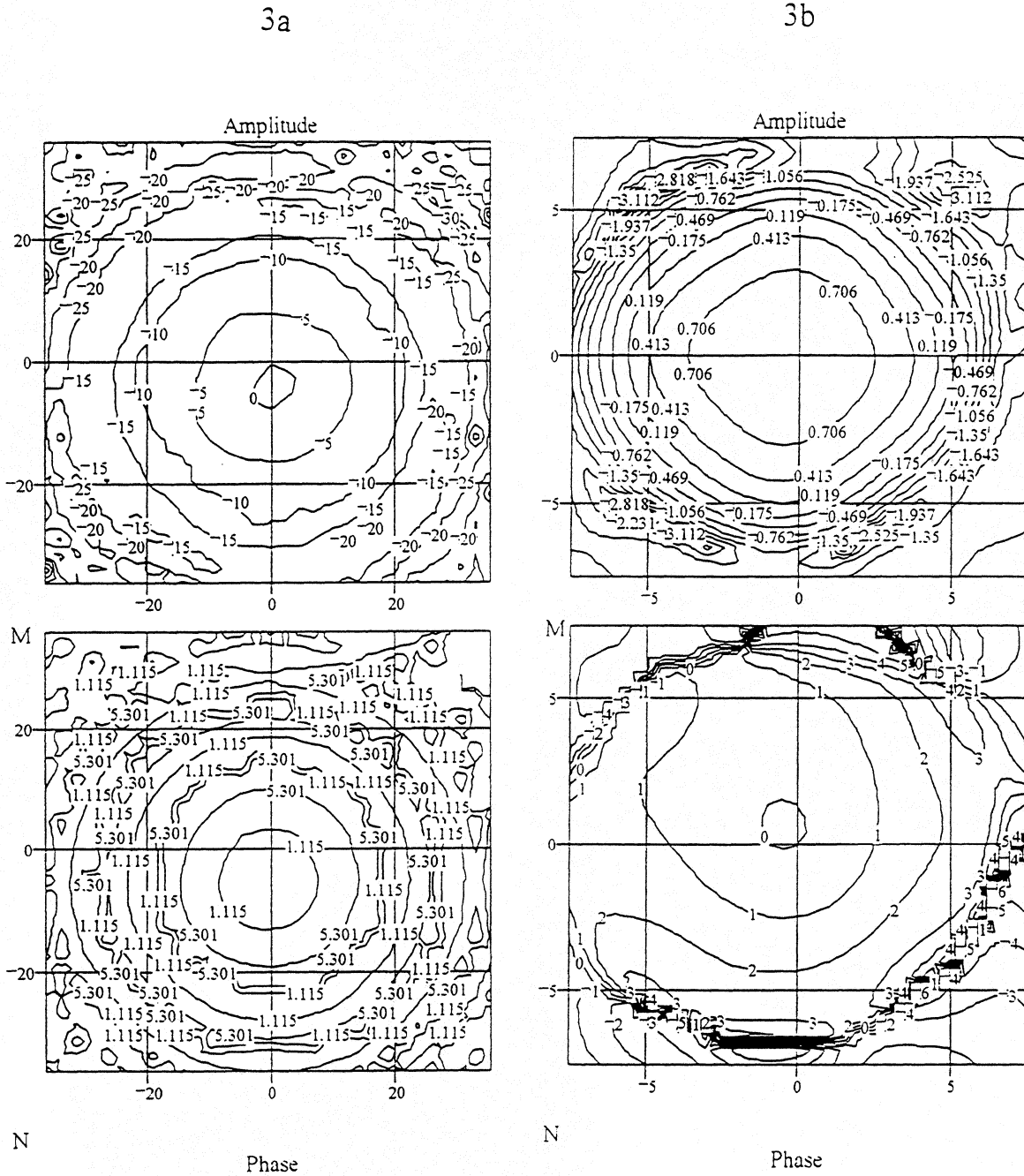


Figure 3: Contour plots of amplitude and phase (a) directly from the raw measurement at 187 GHz, and (b) determined from the theoretical model of the 200 GHz corrugated feed horn at 187 GHz. Amplitude contours are in dB and phase contours in radians.

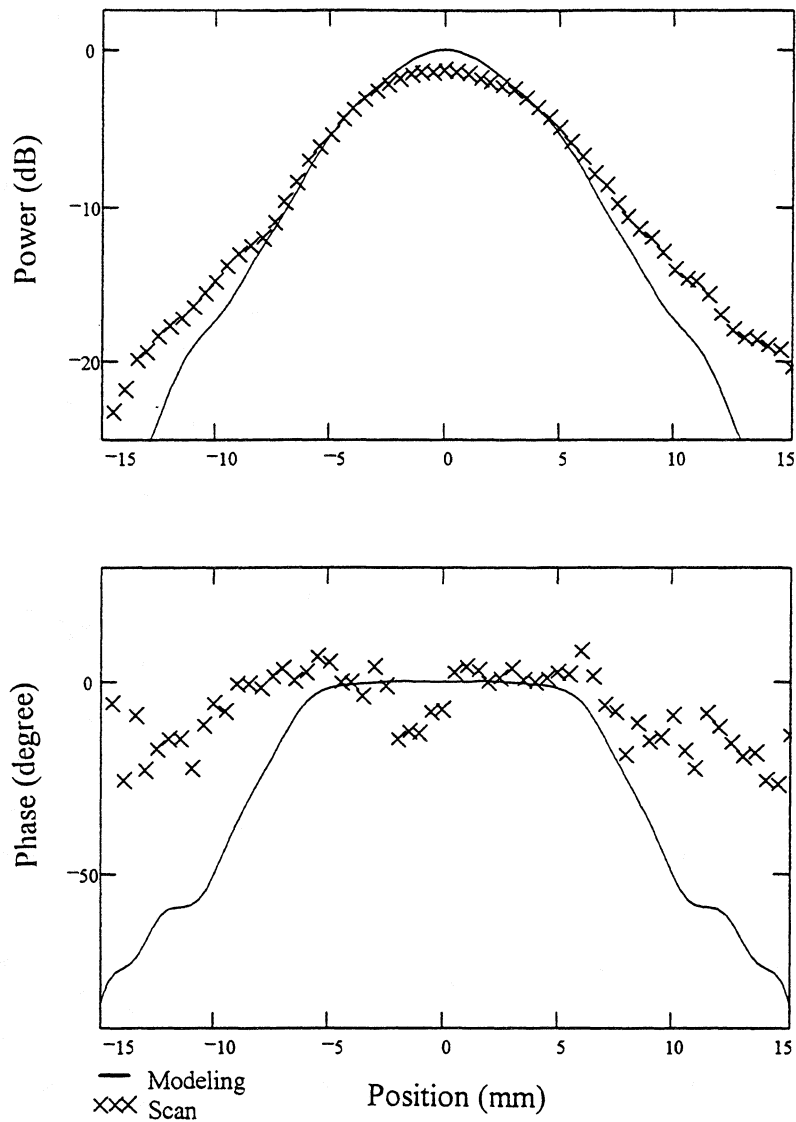


Figure 4: A comparison of the scanned data and the model calculation in the E-plane for the 700 GHz feed horn and lens assembly.

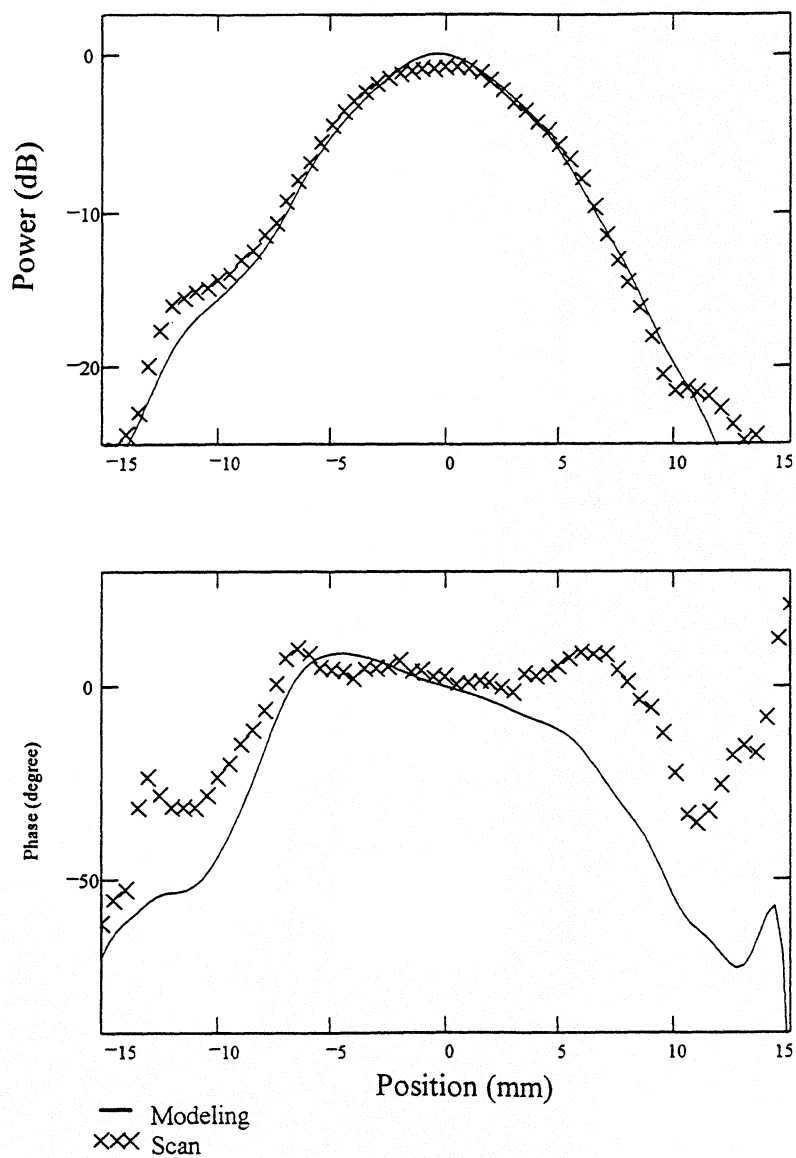


Figure 5: A comparison of the scanned data and the model calculation in the H-plane for the 700 GHz feed horn and lens assembly.